Vol. 81 No. 3 pp. 409–423 ACTA GEOLOGICA SINICA June 2007

# Provenance of Precambrian Fe- and Al-rich Metapelites in the Yenisey Ridge and Kuznetsk Alatau, Siberia: Geochemical Signatures

Igor I. LIKHANOV* and Vladimir V. REVERDATTO

*Institute of Geology and Mineralogy, Siberian Branch, Russian Academy of Sciences, Pr. Acad. Koptyuga, 3, Novosibirsk, 630090, Russian Federation*

**Abstract: Major, trace and rare earth element contents of Fe- and Al-rich metapelites from the Korda (Yenisey Ridge) and Amar (Kuznetsk Alatau) formations were determined to examine the nature, origin and evolution of their protoliths. Results indicate that these rocks are the redeposited and metamorphosed products of Precambrian kaolinitic weathering crusts, while the geochemical distinctions between the studied metapelites are determined by different weathering conditions in the source area and tectonic settings. The protolith of the Korda Formation metapelites was produced by erosion products of the post-Archean granitoid rocks, which accumulated under humid climate conditions in shallow-water basins along the continental margin. The geochemical characteristics of the deeper primary deposits of the Amar Formation suggest that volcanogenic material of mafic composition derived from an island-arc environment had a major role in supplying the erosion zone. These results agree with lithofacies data and with the geodynamic reconstruction of the evolution of the Yenisey Ridge and Kuznetsk Alatau during the Mesoproterozoic and Neoproterozoic, respectively. It was shown that REEs had limited mobility during contact metamorphism. The coherent mobility of REEs during collisional metamorphism may be attributed both to mineral reactions responsible for modal changes and to local chemical heterogeneity inherited from the initial protolith.**

**Key words: geochemistry, protolith, pelitic schists, Kuznetsk Alatau, Yenisey Ridge, Russia**

## 1 Introduction

Numerous findings and generalized statistical whole-rock chemical data show that, as a rule, no radical changes in bulk rock chemical composition (except volatile components such as $H_2O$ and $CO_2$) occur during metamorphism. In the absence of melting, metamorphism produces no drastic changes in the chemical composition of rocks, which preserve defining concentrations of the major elements even under amphibolite and granulite facies conditions, thus testifying to the isochemical nature of metamorphism (e.g. Vernon, 1976, 1998). The preservation of the initial chemical composition of metamorphic rocks allows researchers to infer their primary nature. Dobretsov (1974) developed a methodology and criteria for identifying the primary composition and origin of blueschists based on their whole-rock chemical signatures. In the context of the formational analysis of metamorphic complexes, these approaches were subsequently extrapolated to other types of metamorphic rocks (Golovenok, 1977; Predovsky, 1980).

One of the most effective methods to determine the nature and origin of protoliths and tectonic settings is the analysis of rare earth element (REE) spectra and of indicator ratios between other trace elements. Recent advances in understanding the distribution and geochemistry of the REEs have primarily contributed to a better understanding of the evolution of igneous and sedimentary rocks. Total REE contents in metamorphic rocks have received comparatively little attention. For example, there is virtually no data on the distribution of REEs in Fe- and Al-rich pelitic schists, metamorphism of which leads to the stability of rare mineral assemblages comprising chloritoid, Fe-cordierite and other minerals, such as chloritoid + biotite, chloritoid + biotite + andalusite, and cordierite + garnet + muscovite (Likhanov, 1988a, b, 2003a, b; Likhanov et al., 1998, 1999, 2001a, b). The unusual bulk rock composition is interpreted to have been a distinction between typical metapelite and Fe- and Al-rich metapelite topologies in P-T diagrams (Likhanov

* Corresponding author. E-mail: likh@uiggm.nsc.ru.

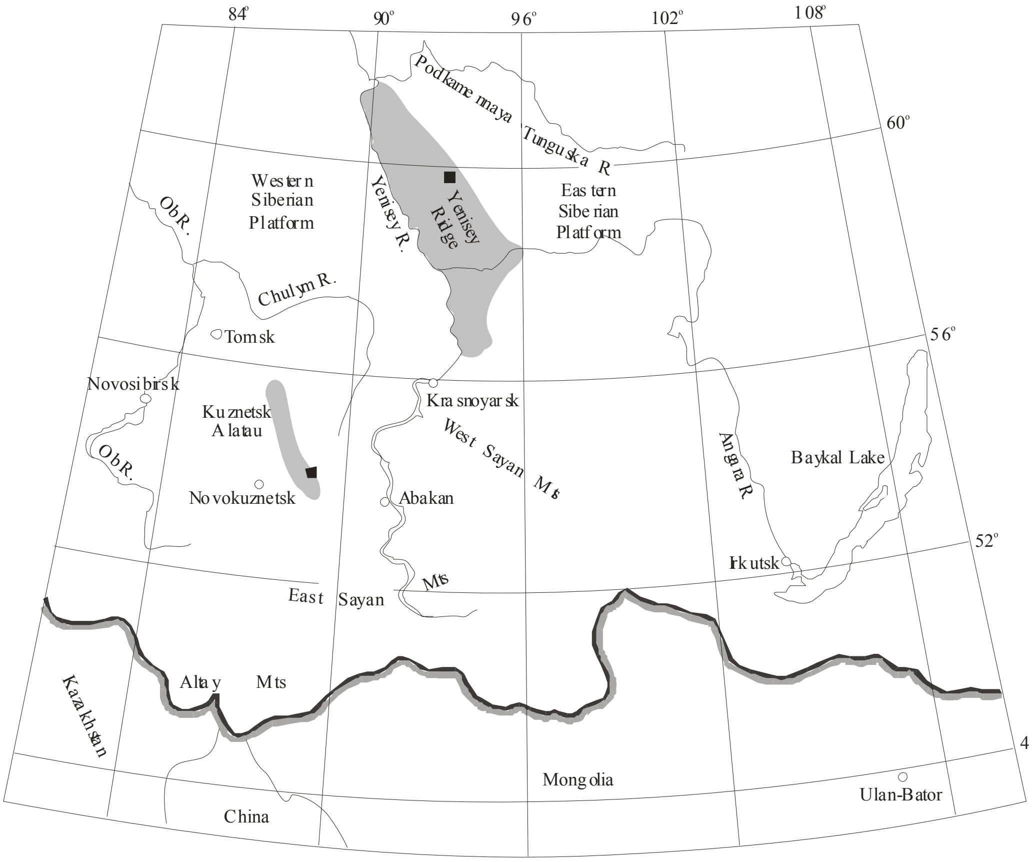


Fig. 1. Regional map showing the location of the studied areas (black squares) in Kuznetsk Alatau (western Siberia) and the Yenisey Ridge (eastern Siberia), Russia.

and Reverdatto, 2004, 2005). In the literature, such a specific Fe- and Al-rich bulk rock composition is attributed to lateritic weathering processes (e.g. Franceschelli et al., 2003; Golovenok, 1977). However, full-profile lateritic weathering crusts are often absent in Precambrian sections (Yudovich and Ketris, 2000), thus arousing interest in the origin of these rocks.

The REE content of a metamorphic rock directly mimics that of the protolith. This assumption has formed the basis for a great number of studies in which the evolution of the protolith was examined in detail without specifically testing for the immobility of the REEs (Grauch, 1989). In this context, the issue of REE migration during metamorphism has been long debated between proponents of isochemical metamorphism and those of metasomatism. The only certainty is that REEs are mobile in certain circumstances (e.g. Cerny et al., 1987; Stahle et al., 1987; Vocke et al., 1987) and immobile in others (Condie, 1993; Cox and Lowe, 1995; McLennan et al., 1995; Rolland et al., 2003). Despite some progress made in this direction, the nature of these circumstances has rarely been determined. Further research on atypical lithologically and chemically distinct types of sample suites may help our understanding of REE contents in metamorphic rocks, because they may contain a record of REE mobility or immobility (Grauch, 1989).

The specific goals of the present paper are: (1) to present and characterize the distribution of major, trace and REEs in pelitic schists, which are simultaneously enriched in iron and aluminum, (2) to clarify the nature and origin of these rocks, with focus on the possible parent rocks that supplied material to the sedimentary precursor of the present-day Fe- and Al-rich pelitic schists, and (3) to determine the specific behavior of REEs in metapelites depending on variations in metamorphic P-T conditions.

## 2 Geological Setting, Mineral Assemblages and Metamorphic Conditions

To address the above-mentioned issues, we studied two rock complexes (Fig. 1) that have been formed through contact and collisional metamorphism. Examination of materials from various geodynamic settings (Reverdatto and Sheplev, 1998), formed under different geothermal gradients (~200 and 1–7 °C/km, respectively) and thermodynamic regimes, allows us to estimate REE patterns as a function of the modal rock composition and P-T conditions under which the rock evolved.

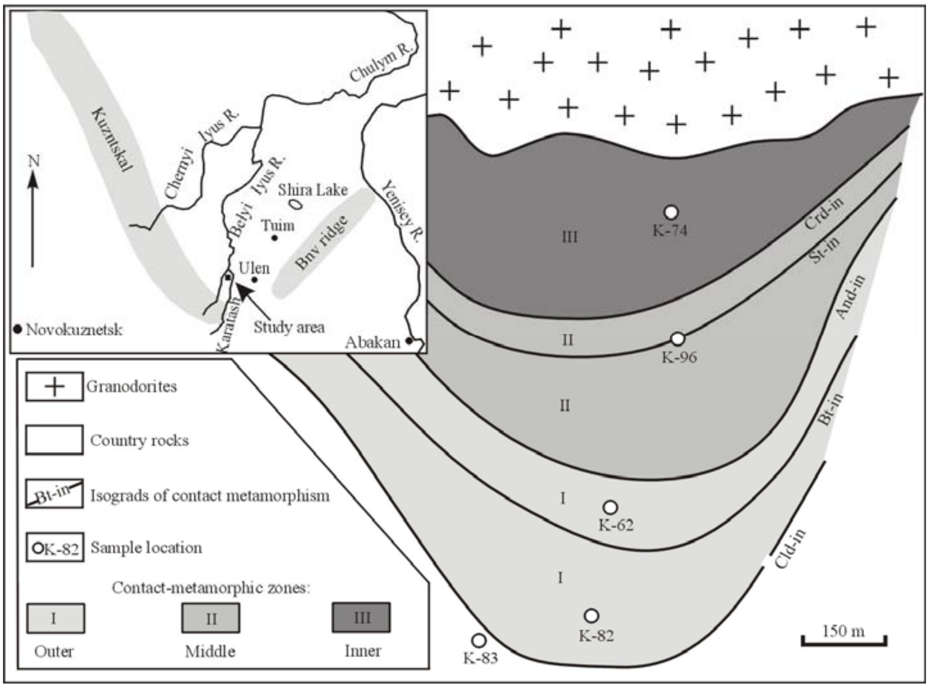


Fig. 2. A schematic geological map of contact metamorphic zones in metapelites of the Amar Formation on the eastern slope of Kuznetsk Alatau.
(1) Granodiorites; (2) country rocks; (3) isograds of contact metamorphism; (4) sample location. Roman numbers (I-III) – zones of contact metamorphism: (I) outer, (II) middle, (III) inner.

The contact aureole of the Karatash granitoid massif is located on the eastern slope of Kuznetsk Alatau, south of the confluence of the Karatash and Bely Iyus rivers (Fig. 2). The host rocks are represented by Neoproterozoic (Upper Vendian, Rb-Sr whole-rock age of 650±25 Ma; Postnikov and Terleev, 2004) deposits of the Amar Formation. They are a green to gray, highly schistose, pelitic phyllites interbedded with thin beds of basic lava and with psammitic and tuff layers that are remarkably uniform both in lithology and chemical composition (Likhanov, 1989). In the study area, the host rocks at the southern contact are regionally metamorphosed to greenschist facies conditions and mainly consist of chlorite-sericite-quartz-hematite metapelites. The contact metamorphic effects of the Karatash intrusive complex with a U-Pb isochron age on zircon of 498±21 Ma (Rublev, 1995) on the pelitic schists are first recognized through the appearance of chloritoid. The thermal aureole, as defined by the chloritoid-in isograd, extends 1.2 km south of the granitoid massif with a distinct zonation marked by changes in the structure of hornfels and in mineral assemblages. Three metamorphic zones and five distinct isograds of contact metamorphism can be distinguished within the contact aureole (Fig. 2). Based on detailed mapping and petrography, the following prograde succession of hornfels mineral assemblages developed with increasing temperatures towards the granitic contact: Cld + Chl + Ms + Qtz + Pl + Pg + Hem + Mag; Cld + Chl + Ms + Qtz + Bt + Rt + Hem (outer zone); And + Bt + Chl + Cld + Ms + Qtz + Pl + Mag; And + Bt + Chl + Ms + Qtz + Pl + St (middle zone); Grt + Crd + Bt + Ms + Pl + Qtz + Mag; Ged + Crd + Bt + PI + Qtz, and Spl + And + Crd + Bt + Ilm (inner zone) (mineral abbreviations after Kretz, 1983). Based on geothermobarometric results (Likhanov, 1988a, b, 1989), regional metamorphism in the country rocks occurred at 380–400 °C, i.e. at temperature corresponding to the greenschist facies. The temperature of contact metamorphism increased towards the intrusive contact from 430 to 640 °C at a constant pressure of 0.31–0.35 GPa, corresponding to the muscovite- and amphibole-hornfels facies (Kolobov et al., 1992; Reverdatto, 1973).

The second study area is located between the Yeruda and Tchirimba Rivers, lying at the eastern margin of the central portion of the Transangarian Yenisey Ridge (Fig. 3). The schematic geological sketch map of this area shows two distinct tectonometamorphic units divided by a thrust zone. The Korda Formation is located SW of the Panimba thrust fault and tectonically underlies the Paleoproterozoic Penchenga Formation to the NE. The Korda Formation represents regionally metamorphosed low-pressure, andalusite-bearing metapelites of Mesoproterozoic age (Middle Riphean Rb-Sr whole-rock age of 1100±50 Ma; Dazenko, 1984; Volobuev et al., 1973) that have been overprinted by Neoproterozoic ($^{40}$Ar-$^{39}$Ar isotopic ages on biotite of 848–851 Ma; Likhanov et al., 2007) of medium-pressure kyanite-bearing assemblages and by textures of collisional metamorphism (Likhanov et al., 2006). A 7 km-wide sheet of medium-pressure rocks is restricted to the NE by the Panimba thrust fault (Fig. 3). Starting approximately 7–8 km southwest of the Panimba thrust fault, the degree of medium-pressure metamorphic overprint the andalusite-bearing rocks and the intensity of deformation in the metapelites increase towards the fault (Likhanov et al., 2000, 2001a). Four distinct metamorphic zones (Fig. 3) can be identified in the Korda Formation. Zone I comprises rocks that were unaffected by the overprint.

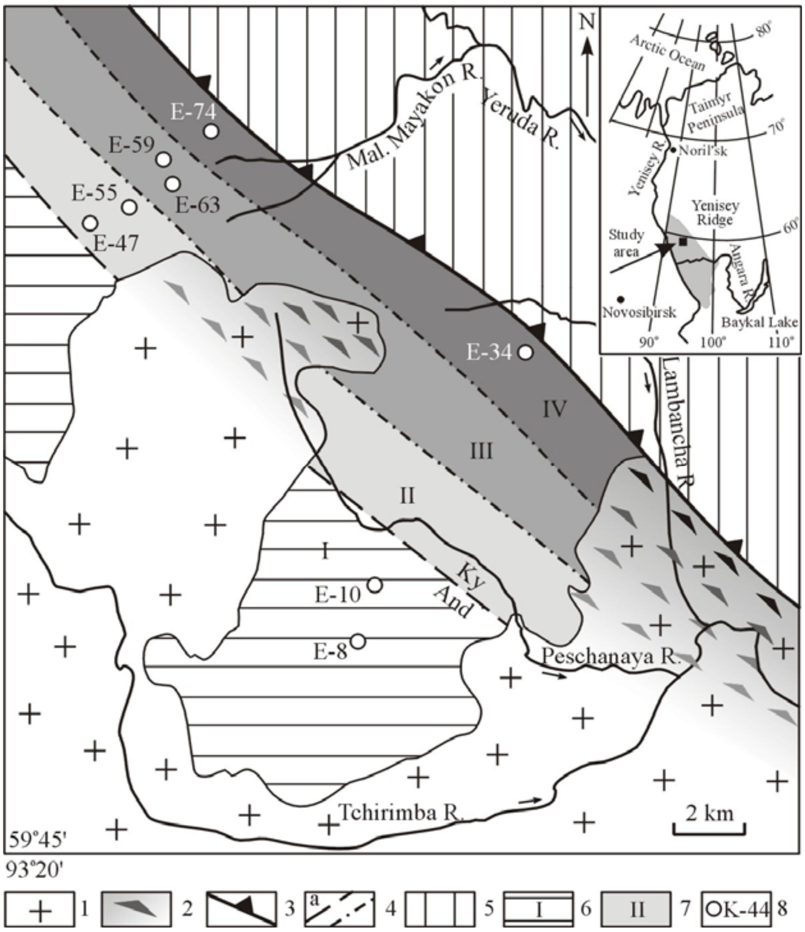


Fig. 3. A geological sketch map of collisional metamorphism on the eastern margin of the central part of the Transangarian region of the Yenisey Ridge in the vicinity of the Panimba thrust.

(1) Granitoids of the Chirimba massif; (2) apogranitic cataclasites and blastocataclasites; (3) Panimba thrust fault; (4) And-Ky isograd (a) and boundaries between zones of metapelites (b); (5) Paleoproterozoic metacarbonates of the Pechenga Formation; (6) Mesoproterozoic regionally-metamorphosed metapelites of the Korda Formation; (7) zones of collisional metamorphism: (II) outer, (III) intermediate, (IV) inner; (8) sample location.

These rocks are mainly characterized by And + Ms + Bt + Cld + Chl + Qtz ± Pl ± Crd mineral assemblages. The boundary between zones I and II coincides with the first appearance of kyanite towards the Panimba thrust fault. All rocks in zones II to IV are characterized by similar mineral assemblages and differ only in their degree and style of deformation. They are represented by Ms + Bt + Chl + Qtz + Grt + St + Ky ± Pl ± Cld ± Sil ± And (relict) mineral assemblages. The other zone boundaries are mainly defined by the style and intensity of deformation, which reflect the progressive obliteration of an early microfabric characterized by an $S_1$ axial planar foliation related to E-vergent $D_1$ isoclinal folds. This foliation is dominant in the Mesoproterozoic low-pressure, andalusite-bearing metamorphic rocks, where it is produced by the preferred orientation of chlorite and mica. Subhorizontal $D_2$ folds with an axial planar $S_2$ crenulation cleavage are superimposed on this early microfabric; the cleavage is weak in low-strain domains but becomes more penetrative in the higher-strain domains near the Panimba thrust. This new foliation represents the main regional fabric element in medium-pressure, kyanite-bearing rocks affected by the Neoproterozoic overprint. Prominent structural features in the medium-pressure rocks are cataclastic deformation and boudinage. Zone II rocks typically show cataclastic breaking of andalusite grains. The grains are locally replaced by kyanite + staurolite + muscovite + quartz pseudomorphs along fractures and margins. The intermediate zone is characterized by more intensively deformed andalusite crystals, which are partially to totally replaced by Ky-St-Ms-Qtz pseudomorphs. Relict andalusite is rarely preserved in the cores of such pseudomorphs. As the Panimba thrust is approached, the last traces of relict andalusite disappear, marking the onset of inner zone IV. Here, adjacent to the Panimba thrust, the degree of deformation increases, resulting in the development of a linear mylonitic fabric and complete recrystallization of minerals to form blastomylonites. The results of geothermobarometry and *P-T* path calculations (Likhanov et al., 2004) indicate that pressure increased toward the Panimba thrust from 0.35–0.4 GPa in zone I through 0.45–0.5 GPa and 0.55–0.6 in zones II and III, respectively, to 0.62–0.67 GPa in zone IV at a relatively constant temperature of 540–600 °C, indicating a surprisingly low geothermal gradient of 1 to 7 °C/km during the Neoproterozoic metamorphic overprint. These results are consistent with metamorphic recrystallization having occurred during thrust emplacement of the tectonically overlying rocks of the Penchenga Formation. Detailed mass-transfer analysis of all mineral reactions which form Ky-St-Ms-Qtz pseudomorphs and minerals in the adjacent matrix were reported by Likhanov and Reverdatto (2002). The calculated mineral reactions are characterized by drastic variations in volume ($-DV$=42%–49%) and minor changes in entropy, and also confirm the possible prograde transformation of andalusite to kyanite and nearly isothermal loading during overthrusting. This indicates that the prograde evolution of chemical and modal mineral compositions during collisional metamorphism was

**Table 1 Whole-rock major element data (wt%), petrochemical modules, and indexes of representative metapelites from the different metamorphic zones**

| | Korda Formation | | | | | | | | Amar Formation | | | | |
|---|---|---|---|---|---|---|---|---|---|---|---|---|---|
| Sample | E-8 | E-10 | E-34 | E-59 | E-55 | E-47 | E-63 | E-74 | K-82 | K-96 | K-83 | K-62 | K-74 |
| $SiO_2$ | 58.3 | 62.6 | 58.6 | 59.7 | 57.3 | 60.2 | 57.2 | 57.1 | 43.4 | 48.6 | 50.6 | 46.0 | 48.2 |
| $TiO_2$ | 0.86 | 0.95 | 0.58 | 0.96 | 1.06 | 0.94 | 0.95 | 0.86 | 1.20 | 1.03 | 1.16 | 1.4 | 1.22 |
| $Al_2O_3$ | 21.5 | 18.3 | 21.7 | 20.4 | 21.3 | 19.1 | 24.7 | 22.7 | 26.7 | 23.7 | 22.6 | 30.0 | 27.0 |
| $Fe_2O_3$ | 8.29 | 8.64 | 9.01 | 7.48 | 9.15 | 10.3 | 7.96 | 9.63 | 18.0 | 15.2 | 13.5 | 10.7 | 15.7 |
| MnO | 0.07 | 0.07 | 0.15 | 0.03 | 0.25 | 0.11 | 0.05 | 0.04 | 0.11 | 0.04 | 0.14 | 0.07 | 0.08 |
| MgO | 1.54 | 2.81 | 2.81 | 1.89 | 1.53 | 1.92 | 2.03 | 1.52 | 4.10 | 2.70 | 3.26 | 1.49 | 1.96 |
| CaO | 0.23 | 0.20 | 1.06 | 0.27 | 0.34 | 0.24 | 0.31 | 0.31 | 0.54 | 0.40 | 0.67 | 0.54 | 0.38 |
| $Na_2O$ | 0.30 | 0.29 | 0.30 | 0.48 | 1.13 | 0.31 | 0.48 | 0.29 | 0.72 | 1.40 | 1.24 | 2.00 | 0.90 |
| $K_2O$ | 3.24 | 2.91 | 2.12 | 3.01 | 3.29 | 3.08 | 2.52 | 2.67 | 0.29 | 2.30 | 1.00 | 1.29 | 0.57 |
| LOI | 5.29 | 2.61 | 2.73 | 4.83 | 4.58 | 3.79 | 2.94 | 4.87 | 6.51 | 5.75 | 6.46 | 6.41 | 5.18 |
| Total | 99.6 | 99.4 | 99.0 | 99.1 | 99.9 | 100.0 | 99.1 | 100.0 | 100.1 | 100.2 | 99.9 | 99.4 | 100.6 |
| HM | 0.53 | 0.45 | 0.53 | 0.48 | 0.55 | 0.50 | 0.59 | 0.58 | 1.02 | 0.80 | 0.72 | 0.90 | 0.89 |
| ASM | 0.37 | 0.29 | 0.37 | 0.34 | 0.37 | 0.32 | 0.43 | 0.40 | 0.62 | 0.49 | 0.45 | 0.65 | 0.56 |
| FM | 0.17 | 0.18 | 0.20 | 0.16 | 0.19 | 0.20 | 0.17 | 0.20 | 0.47 | 0.35 | 0.31 | 0.25 | 0.34 |
| TM | 0.04 | 0.05 | 0.03 | 0.05 | 0.05 | 0.05 | 0.04 | 0.04 | 0.05 | 0.04 | 0.05 | 0.05 | 0.05 |
| PM | 0.15 | 0.16 | 0.10 | 0.15 | 0.15 | 0.16 | 0.10 | 0.12 | 0.01 | 0.10 | 0.04 | 0.04 | 0.02 |
| AM | 0.09 | 0.10 | 0.14 | 0.16 | 0.34 | 0.10 | 0.19 | 0.11 | 2.48 | 0.61 | 1.24 | 1.55 | 1.58 |
| NAM | 0.16 | 0.18 | 0.11 | 0.17 | 0.21 | 0.18 | 0.12 | 0.13 | 0.04 | 0.16 | 0.10 | 0.11 | 0.05 |
| IM | 0.37 | 0.45 | 0.41 | 0.35 | 0.42 | 0.52 | 0.31 | 0.41 | 0.59 | 0.57 | 0.54 | 0.33 | 0.52 |
| CIA | 82.9 | 82.1 | 82.1 | 81.8 | 77.9 | 81.7 | 85.8 | 85.2 | 91.5 | 81.1 | 83.9 | 84.1 | 90.6 |
| CIW | 95.9 | 95.6 | 89.9 | 94.1 | 89.6 | 95.3 | 94.8 | 95.6 | 92.5 | 88.7 | 87.4 | 87.5 | 92.6 |
| ICV | 0.68 | 0.97 | 0.84 | 0.75 | 0.81 | 0.89 | 0.63 | 0.66 | 0.97 | 0.99 | 1.00 | 0.6 | 0.72 |
| PIA | 95.2 | 94.7 | 88.9 | 93.1 | 87.7 | 94.3 | 94.2 | 95.0 | 92.4 | 87.5 | 86.9 | 87.0 | 92.4 |

Total iron as $Fe_2O_3$. LOI, loss on ignition. See the text for abbreviations of modules and indexes.

controlled by a gradual pressure increase (at nearly constant temperature) accompanied by deformation within the bulk composition of the protolith (Likhanov and Reverdatto, 2002; Korobeinikov et al., 2006).

## 3 Sampling and Analytical Methods

To study the behavior of materials during contact and collisional metamorphism, a total of 13 rock samples were collected from different metamorphic zones with available reliable P-T estimates and data on the modal composition of rocks. The mineral assemblages of investigated rocks are typical of the zones from which they were sampled. Sample locations are shown in Figs. 2 and 3. Bulk rock analyses were obtained by XRF using a VRA-20R energy dispersive spectrometer (Carl Zeiss, Jena, Germany) at the United Institute of Geology, Geophysics and Mineralogy (UIGGM) in Novosibirsk. LOI values were determined by ordinary measuring weight loss at 1000 °C. The detection limits for the majority of rock-forming components were 0.02–0.005%; only MgO and $Na_2O$ had detection limits of 0.05 and 0.1%, respectively. Results are reported in Table 1.

Trace and rare-earth elements (14 REEs, Sc, Ni, Co, Rb, Sr, Y, Zr, Nb, Cs, Ba, Hf, Ta, Th, U) were measured by ICP-MS using a VG Element PQ2 (Germany) analyzer in the UIGGM Laboratory of Analytical Geochemistry. Powdered metapelite samples, each weighing about 100 mg, were decomposed by fusion with Li metaborate at 1000 °C, followed by dissolution in 5% nitric acid with an initial sample dilution coefficient of 6250.The internal standard was $^{115}In$, which was added to the diluted solution. The external standard and blank solution were measured every five samples to monitor instrumental fluctuations and control the cleanliness of the system that supplies the sample solution to the device. The external standards were BCR-1 and JB-3 (Geological Survey of the USA and Japan). Data are reported in Table 2.

## 4 Results and Discussion

### 4.1 Bulk-rock chemistry and isochemical nature of metamorphism

As shown in Table 1, the studied rocks are classified as metapelites enriched in both iron and alumina (Hoschek, 1969). These rocks have high-Fe ($X_{Fe}$ = FeO/(FeO+MgO+MnO) = 0.65–0.85 whole rock on a mole basis) and high-Al ($X_{Al}$ = $Al_2O_3$−3$K_2O$/($Al_2O_3$−3$K_2O$+FeO+MgO+ MnO) = 0.3–0.6) bulk compositions with respect to the average pelite whole-rock compositions ($X_{Fe}$ = 0.52 and $X_{Al}$ = 0.13) (Shaw, 1956; Symmes and Ferry, 1992) and to PAAS (post-Archean Australian schists) (Taylor and McLennan, 1985). In the AFM projection of Thompson (1957) they are plotted above the garnet-chlorite tie-line (Fig. 4). Compared to the average pelitic rock compositions reported by Ague (1991), the investigated rocks are more depleted in $K_2O$, CaO and $Na_2O$. Along with the indicated higher contents of total iron and alumina, the metapelites of the Amar Formation have higher $TiO_2$ and MgO and lower $SiO_2$, CaO and $K_2O$ contents than the PAAS; the $Na_2O$ content varies considerably from 0.72 to 2 wt% in the different

**Table 2 Trace and REE contents (ppm) and their elemental ratios for metapelites from the different metamorphic zones**

| | Korda Formation | | | | | | | | Amar Formation | | | | |
|---|---|---|---|---|---|---|---|---|---|---|---|---|---|
| Sample | E-8 | E-10 | E-34 | E-74 | E-55 | E-47 | E-63 | E-59 | K-82 | K-96 | K-83 | K-62 | K-74 |
| La | 70 | 85 | 12 | 16 | 69 | 70 | 30 | 33 | 16 | 31 | 34 | 18 | 21 |
| Ce | 119 | 154 | 36 | 33 | 115 | 130 | 57 | 76 | 25 | 60 | 43 | 28 | 52 |
| Pr | 17 | 22 | 4 | 4.1 | 18 | 18 | 7.6 | 8.6 | 3.9 | 7.6 | 5.6 | 4.1 | 7.2 |
| Nd | 56 | 73 | 13 | 14 | 57 | 58.9 | 25 | 28 | 16 | 29 | 19 | 24 | 29 |
| Sm | 10 | 13 | 2.6 | 2.7 | 11 | 10 | 4.5 | 5.2 | 3.9 | 8 | 4.2 | 6.7 | 5.8 |
| Eu | 1.8 | 2.2 | 0.69 | 0.67 | 2 | 1.9 | 0.91 | 0.96 | 1.3 | 2.3 | 1.2 | 1.4 | 1.7 |
| Gd | 8.9 | 10 | 2.4 | 2.4 | 9.8 | 8.9 | 4.3 | 4.7 | 5 | 11 | 6.8 | 9.4 | 7.7 |
| Tb | 1.3 | 1.3 | 0.49 | 0.38 | 1.5 | 1.2 | 0.64 | 0.74 | 0.87 | 1.7 | 0.64 | 1.12 | 0.94 |
| Dy | 7.5 | 7.1 | 3.6 | 2.4 | 9.2 | 7 | 4 | 4.5 | 6.1 | 11 | 7.4 | 9.3 | 9.4 |
| Ho | 1.5 | 1.3 | 0.82 | 0.5 | 1.8 | 1.4 | 0.85 | 0.91 | 1.4 | 2.4 | 1.7 | 1.6 | 1.9 |
| Er | 4.5 | 3.8 | 2.7 | 1.7 | 4.9 | 4 | 2.6 | 2.7 | 4.3 | 6.4 | 4.4 | 4.9 | 7.1 |
| Tm | 0.71 | 0.59 | 0.49 | 0.31 | 0.79 | 0.63 | 0.43 | 0.46 | 0.72 | 1.2 | 0.91 | 0.77 | 0.89 |
| Yb | 4.5 | 3.7 | 3.2 | 2.1 | 4.8 | 4.1 | 2.7 | 3.1 | 4.7 | 5.5 | 4.9 | 7.1 | 6.3 |
| Lu | 0.68 | 0.52 | 0.49 | 0.36 | 0.68 | 0.63 | 0.4 | 0.46 | 0.75 | 1.1 | 0.98 | 0.87 | 1.02 |
| Sc | 18 | 16 | 19 | 23 | 16 | 21 | 24 | 23 | 56 | 60 | 62 | 59 | 60 |
| Co | 8.1 | 10 | 11 | 16 | 14 | 13 | 11 | 14 | 27 | 27 | 29 | 28 | 28 |
| Ni | 16 | 19 | 18 | 29 | 18 | 22 | 21 | 30 | 60 | 63 | 59 | 62 | 63 |
| Rb | 143 | 127 | 143 | 141 | 130 | 125 | 103 | 121 | 8.5 | 25 | 14 | 19 | 21 |
| Sr | 90 | 94 | 101 | 87 | 127 | 112 | 119 | 120 | 210 | 480 | 319 | 421 | 460 |
| Y | 38 | 36 | 34 | 30 | 42 | 37 | 31 | 37 | 60 | 74 | 66 | 72 | 71 |
| Zr | 217 | 219 | 226 | 238 | 249 | 224 | 231 | 237 | 173 | 190 | 178 | 181 | 180 |
| Nb | 15 | 17 | 18 | 15 | 23 | 21 | 19 | 18 | 8.1 | 8.8 | 8.5 | 8.3 | 8.6 |
| Cs | 6.0 | 5.4 | 5.1 | 4.2 | 6.0 | 5.3 | 5.8 | 5.4 | 1.0 | 2.4 | 1.4 | 1.7 | 2.3 |
| Ba | 400 | 511 | 478 | 492 | 570 | 524 | 598 | 570 | 155 | 274 | 188 | 211 | 256 |
| Hf | 7.2 | 7.1 | 7.3 | 6.6 | 7.6 | 7.4 | 6.9 | 6.7 | 5.2 | 5.9 | 5.6 | 5.7 | 5.5 |
| Ta | 1.3 | 1.4 | 1.7 | 1.5 | 1.9 | 1.6 | 1.6 | 1.7 | 0.36 | 0.49 | 0.44 | 0.48 | 0.46 |
| Th | 18 | 21 | 20 | 24 | 22 | 23 | 23 | 24 | 3.3 | 4.1 | 3.7 | 3.9 | 4.0 |
| U | 2.7 | 2.8 | 3.1 | 2.1 | 3.1 | 2.0 | 2.4 | 2.7 | 4.0 | 4.8 | 4.7 | 4.3 | 4.7 |
| $(La/Yb)_n$ | 10.7 | 17 | 2.54 | 4.62 | 10.5 | 11.5 | 7.79 | 7.45 | 2.22 | 2.93 | 3.60 | 2.15 | 2.14 |
| $(Gd/Yb)_n$ | 1.63 | 2.39 | 0.61 | 0.83 | 1.79 | 1.76 | 1.34 | 1.27 | 0.83 | 1.24 | 0.86 | 1.34 | 0.94 |
| Eu/Eu* | 0.57 | 0.57 | 0.83 | 0.79 | 0.58 | 0.60 | 0.62 | 0.58 | 0.90 | 0.75 | 0.68 | 0.54 | 0.78 |
| Ce/Ce* | 0.81 | 0.84 | 1.25 | 0.96 | 0.77 | 0.86 | 0.89 | 1.06 | 0.74 | 0.87 | 0.68 | 0.76 | 0.89 |
| $(LREE/HREE)_n$ | 3.42 | 4.72 | 1.50 | 2.31 | 3.08 | 3.82 | 2.79 | 2.95 | 0.98 | 1.19 | 1.38 | 0.91 | 1.18 |
| Total REE | 303 | 378 | 82.5 | 80.6 | 306 | 317 | 141 | 169 | 89.9 | 178 | 135 | 117 | 152 |
| La/Sc | 3.89 | 5.31 | 0.63 | 0.70 | 4.31 | 3.33 | 1.25 | 1.43 | 0.29 | 0.52 | 0.55 | 0.31 | 0.35 |
| Th/Sc | 1.00 | 1.31 | 1.05 | 1.04 | 1.38 | 1.10 | 0.96 | 1.04 | 0.06 | 0.07 | 0.06 | 0.07 | 0.07 |
| La/Th | 3.89 | 4.05 | 0.6 | 0.67 | 3.14 | 3.04 | 1.30 | 1.38 | 4.85 | 7.56 | 9.19 | 4.62 | 5.25 |
| Co/Th | 0.45 | 0.48 | 0.55 | 0.67 | 0.64 | 0.57 | 0.48 | 0.58 | 8.18 | 6.59 | 7.84 | 7.18 | 7.00 |
| Th/U | 6.67 | 7.5 | 6.45 | 11.4 | 7.10 | 11.5 | 9.58 | 8.89 | 0.83 | 0.85 | 0.79 | 0.91 | 0.85 |

metamorphic zones. In an earlier paper, the authors (Likhanov, 2003b) carried out a statistical analysis of the country and contact metamorphic rocks of the Amar Formation, by comparing the mean values and dispersion of the whole-rock major elements between hornfelses and unaltered schists using Student's t- and Fisher's F-tests (Likhanov, 2003b), and following the methods described by Urbakh (1964). These data reveal that hornfelses and country rocks have an identical composition for all elements (except FeO and $Fe_2O_3$) at the 95% significance level. The difference in FeO and $Fe_2O_3$ content between hornfelses and country rocks may be determined by reducing conditions during contact metamorphism (Yugster, 1961).

The Korda Formation metapelites have nearly the same $SiO_2$, MnO, and $K_2O$ contents and $TiO_2$, MgO, CaO, and $Na_2O$ contents being somewhat lower than the PAAS. They differ from the Amar metapelites by lower concentrations of most petrogenic components except $SiO_2$ and $K_2O$. A selection of whole-rock data (Table 1) on Korda Formation metapelites from the four different zones reveals that $SiO_2$ (57.1–62.6 wt%), $Fe_2O_3$ (7.48–10.3 wt%), $Na_2O$ (0.29–1.13 wt%) and CaO (0.2–1.06 wt%) contents show the greatest variability. Such changes are probably related to local variations in the relative abundance of quartz-rich and extremely mica-rich layers within the samples, and in the modal amounts of plagioclase and carbonate. Average whole-rock data and standard deviations for metapelites from different zones were reported in a previous work (Likhanov and Reverdatto, 2002). These data confirm that rocks from different metamorphic zones have nearly identical major element compositions (overlap within errors). Although there are negligible differences in FeO and MgO concentrations among the samples, these are not systematically related to metamorphic grade and maybe have been caused by some local heterogeneity inherited from the initial protolith.

Because isochemical suites of the metapelitic rocks are available, differences between mineral assemblages from different metamorphic zones can be attributed to changes in intensive variables rather than changes in bulk rock composition.

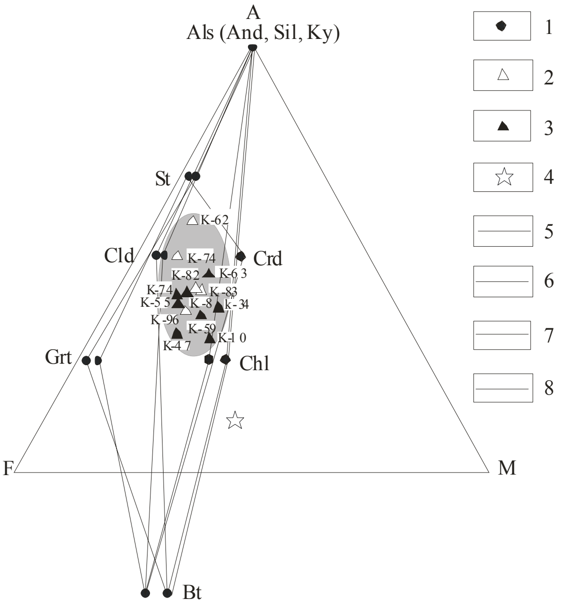

Fig. 4. AFM phase diagram (Thompson, 1957) representing the chemical compositions of rocks and minerals, and typical mineral assemblages of Fe- and Al-rich metapelites.

For all rocks the projection was constructed from Ms, Qtz, Pl and a fluid with a constant $a_{H2O}$. (1) Projected mineral compositions; (2–3) projected bulk compositions of samples from the Amar (2) and Korda (3) formations; (4) average low-grade typical pelite of Shaw (1956) and Symmes and Ferry (1992); mineral assem-blages: (5) low-pressure metapelites of the Korda Formation from zone I, (6) medium-pressure metapelites of the Korda Formation from zones II-IV, (7) low-grade metapelites of the Amar Formation from the outer and middle zones, (8) high-temperature hornfels from the inner zone of the contact aureole. The shaded ellipse represents the field of bulk rock compositions of Fe- and Al-rich metapelites.

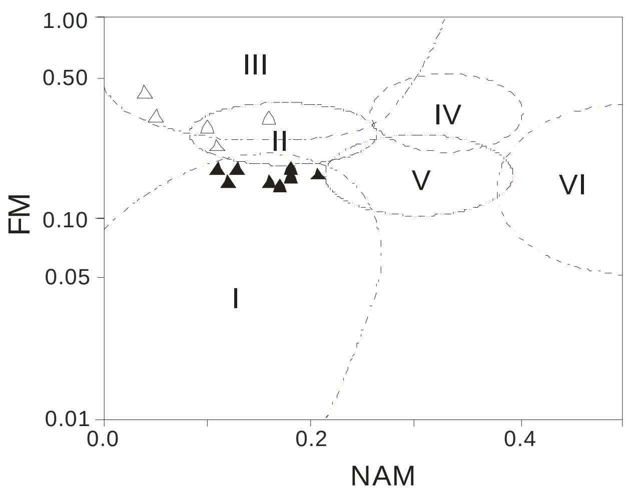

Fig. 5. Data points of Amar Formation (open triangles) and Korda Formation (black triangles) metapelites plotted in the FM-NAM module diagram (Yudovich and Ketris, 2000).

FM represented on a logarithmic scale. Predominent clay minerals in the fields are: (I) kaolinite, (II) montmorillonite with minor abundance of kaolinite and hydromica, (III) chlorite with minor abundance of Fe-hydromica, (IV) chlorite and hydromica, (V) chlorite, smectite and hydromica, (VI) hydromica with appreciable amount of potassium feldspar.

**4.2 Major element geochemistry and nature of the protolith**

To reconstruct the composition of the protolith, weathering conditions, and the paleogeographic and paleoclimatic setting of the environments, we used a system of petrochemical modules and genetic diagrams (Yudovich and Ketris, 2000; Predovsky, 1980) with the well-known ratios: Chemical Index of Alteration (CIA = $[Al_2O_3/(Al_2O_3 + CaO + Na_2O + K_2O)]\cdot 100$), (Nesbitt and Young, 1982; Visser and Young, 1990); Chemical Index of Weathering (CIW = $[Al_2O_3/(Al_2O_3 + CaO + Na_2O)]\cdot 100$), (Harnois, 1988); Index of Compositional Variability (ICV = $(Fe_2O_3 + K_2O + Na_2O + CaO + MgO + TiO_2)/Al_2O_3$), (Cox et al., 1995); and Plagioclase Index of Alteration (PIA = $[(Al_2O_3 - K_2O)/(Al_2O_3 + CaO + Na_2O + K_2O)]\cdot 100$), (Fedo et al., 1995) (Table 1).

Metapelites of the Amar Formation are characterized by the following values of specific geochemical features: the hydrolyzate module, HM = $(Al_2O_3 + TiO_2 + \Sigma Fe_2O_3 + MnO)/SiO_2$, ranges from 0.72 to 1.02; the iron module, IM = $(\Sigma Fe_2O_3 + MnO)/SiO_2$, is approximately 0.55; the Al-Si module, ASM = $Al_2O_3/SiO_2$, varies from 0.45 to 0.65; and the femic module, FM = $(\Sigma Fe_2O_3 + MnO + MgO)/SiO_2$, ranges from 0.25 to 0.47. Thus, the metapelites can be classified as hypo-, normo-, and pseudohydrolyzates (Yudovich and Ketris, 2000). The alkalinity module, AM = $Na_2O/K_2O$, varies from 0.61 to 2.48, while the potassium module, PM = $K_2O/Al_2O_3$, is less than 0.10. These two values suggest that the primary sediments were enriched in chlorite and plagioclase, with an admixture of kaolinite. The high $Na_2O$ (up to 2 wt%) and MgO (up to 4 wt%) concentrations testify to the presence of basic pyrogenic admixture and the prevalence of montmorillonite in the protolith mineral composition. This conclusion is supported by XRD clay mineral patterns (Nasedkina, 1981) and the FM-NAM relationship, where NAM stands for the normalized alkalinity module, i.e., NAM = $(Na_2O + K_2O)/(Al_2O_3)$ (Yudovich and Ketris, 2000). In the FM-NAM diagram, some data points fall within the field of chlorite with Fe-hydromicas, while other data points are located near the field of montmorillonite-rich clays with kaolinite and hydromica (Fig. 5). For comparison, in the FAK diagram of Predovsky (1980) with the coordinates F = $(\Sigma Fe_2O_3 + MgO)/SiO_2$, A = $A_2O_3-K_2O-Na_2O-CaO$ and K = $K_2O-Na_2O$, these rocks are concentrated in the area of overlap between graywackes and hydromicaceous clays (Likhanov, 2003b; here this plot is omitted.). Specific ferruginous products of the alteration of basic volcanic rocks and their tuffs were therefore involved in the intense erosion of the kaolinitic weathering crust. The weathering crusts of basic and intermediate rocks were also washed out, as indicated by the data on the primary composition of the initial rocks, by the high ASM, FM and AM values, by the positive correlation between IM and FM, and by the presence of fragments of weathered effusives (Savko and Dodatko, 1991). The poor sorting and low degree of roundness of clastic material may be related to an insignificant transport of erosion products from the source area. Primary clay minerals were recrystallized and replaced by Fe-chlorite and sericite during low-grade regional metamorphism.

The Korda Formation metapelites typically have low HM (0.45–0.59), IM (0.31–0.52), ASM (0.29–0.43), and FM (0.16–0.20) values relative to the Amar Formation metapelites, suggesting that they are an association of normal siallites and supersiallites (clay rocks) according to the classification of Yudovich and Ketris (2000). AM (0.09–0.19) and PM (0.1–0.16) values suggest the predominance of hydromica and chlorite in the source clayey material. However, in the FM-NAM (Yudovich and Ketris, 2000) and FAK (Predovsky, 1980) diagrams these rocks fall within the compositional field of kaolinite (Fig. 5), that may have been caused by paleogeographic conditions during sedimentation (Likhanov, 2003b). Kaolinite clays may have been accumulated near the continental-margin zone, while the more fine-grained clay material of chlorite-hydromica composition was deposited in offshore marine basins. The lower alkalinity (NAM = 0.11–0.21), along with the low MgO values (< 3 wt%) and higher $K_2O$ contents (> 3 wt%), results from the presence of K-rich granitoids in the detrital material of erosion products and is indicative of no admixture of basic volcanic rocks. The values of the titanic module (TM = $TiO_2/Al_2O_3$ = 0.03–0.05) are typical of initial sediment accumulation in shallow nearshore basins under humid climate conditions, thus closely matching the lithofacies data (Akul'shina, 1980).

Plots in the FM-NAM (Yudovich and Ketris, 2000) and FAK (Predovsky, 1980) diagrams, as well as high CIA, CIW, and PIA values (77.9–95.9) and low ICV values (<1), indicate that these sediments were derived from an intensely weathered source area of the studied outcrops. The ferruginous-aluminous metapelites primarily represent redeposited and metamorphosed products of Precambrian kaolinitic, rather than lateritic, weathering crusts. In Kuznetsk Alatau and the Yenisey Ridge, the chemical weathering of rocks during the Mesoproterozoic (Middle Riphean) and Neoproterozoic (Vendian) did not reach the lateritization stage, with the final formation of decomposition products of aluminosilicates. Weathering was mainly limited by the predominant formation of kaolinite-montmorillonite-chlorite-hydromica rocks.

### 4.3 Trace element geochemistry and geodynamic interpretations

There are strong compositional differences between altered rocks derived from granitic "continental" sources and those derived from mafic sources. The trace element behavior is believed by many geologists to be the best indicators for these reconstructions, because they are not significantly redistributed during weathering, transport, diagenesis, and metamorphism (Cox and Lowe, 1995). As a result, their abundance in altered rocks generally reflects the composition of the source rocks, thus allowing us to judge about their protolith origin. The major differences between the weathering products of different crystalline source rocks are summarized below.

The REE pattern are commonly evaluated based on the following parameters: the total REE content; the $(LREE/HREE)_n$ ratio, an indicator of paleoclimate (Balashov, 1976); the ratio $Eu/Eu^* = Eu_n(Sm_n + Gd_n)\cdot 0.5$ (Jahn and Condie, 1995) and the ratio $Ce/Ce^* = Ce_n(Ln_n + Pr_n)\cdot 0.5$, an indicator of sedimentation environments (Murray et al., 1990, 1991); the $(La/Yb)_n$ ratio, the general slope of the REEs distribution spectrum (Wronkiewicz and Condie, 1990); and the $(Gd/Yb)_n$ ratio, an indicator of the degree of HREE depletion. The latter parameter is primarily controlled by the provenance rock composition and local tectonics (Condie, 1993). The REE and trace element contents, as well as diagnostic elemental ratios (La/Sc, Th/Sc, La/Th, Co/Th, and Th/U), which are very informative on the composition and formation conditions of the protolith (Holail and Mogzahi, 1998; Lee, 2002; Sifeta et al., 2005), are reported in Table 2.

The chondrite-normalized REE distribution spectra of all samples from the Amar Formation (Fig. 6a) show a negative Eu anomaly ($Eu/Eu^*$ = 0.54–0.90) similar to that of the PAAS (Taylor and McLennan, 1985). The Amar Formation metapelites are characterized by lower values of the following geochemical parameters (Table 2): $(La/Yb)_n$ = 2.14–3.60, $(Gd/Yb)_n$ = 0.83–1.33, and $(LREE/HREE)_n$ = 0.91–1.38 with respect to PAAS compositions. The total REE content varies from 89 to 178 ppm. These data reflect the involvement of large volumes of products of basic volcanism in the erosion zone, and indeed these REE distribution spectra are generally similar to those of tholeiitic island arc basalts. This assumption is consistent with specific features of REEs fractionation involving the loss of LREEs and gain of HREEs during the weathering of basic rocks (Podporina, 1985). It is also confirmed by petrochemical features of rocks and by lithofacies data (Nasedkina, 1981).

The Amar Formation metapelites are significantly depleted in lithophile (Rb, Cs, Ba) elements and high-field strength elements (HFSEs – Zr, Hf, Ta, Nb, Th) and

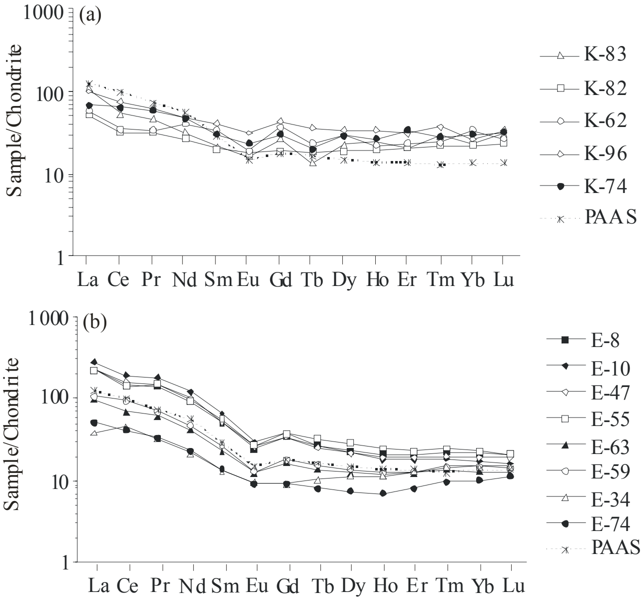


Fig. 6. Chondrite-normalized REE patterns for the rocks of the Amar (a) and Korda (b) formations.

Sample are numbered (from the bottom upwards) according to increasing temperatures (a) and pressures (b).

enriched in U, Y, Sr as compared with PAAS and the average upper continental crust (Table 2). The transitional metal concentrations (Sc, Co, Ni) are somewhat higher than in PAAS. The inheritance of the primary magmatic composition is confirmed by a high positive linear correlation between the contents of HFSEs – Zr, Hf, Y, Ta, and Nb (Table 2). These geochemical peculiarities suggest the supply of mantle material into the sedimentary basin occurred at about 900–800 Ma ago (Postnikov and Terleev, 2004). The low $(LREE/HREE)_n$ (0.91–1.38) and $Ce/Ce^*$ (< 0.9) values (Murray et al., 1990, 1991) likely indicate the deep-water basin sedimentation environments of initial protolith for the Amar Formation metapelites. With respect to average PAAS ratios, these samples display lower La/Sc (0.29–0.55), Th/Sc (0.06–0.07), and Th/U (6.45–11.4) ratios and higher La/Th (4.62–9.19) and Co/Th (6.59–8.18) ratios, thereby indicating the erosion of basic volcanic rocks. The primary island arc tholeiites and basalts nature of the rocks can also be implied from the Zr-Nb-Y (Meschide, 1986) and Hf-Th-Ta (Wood, 1980) diagrams, which permit to distinguish the tectonic settings for basic volcanic rocks (Likhanov et al., 2005; here these plots are omitted.). This conclusion is supported by reviewing the data points in the discriminant Th-Co-Zr and La-Th-Sc diagrams (Bhatia and Crook, 1986) for classifying tectonic settings in which graywackes were accumulated (Fig. 7). Hence, island-arc and oceanic settings prevailed during the formation of basic volcanic rocks in the erosion zone. These geodynamic reconstructions are consistent with the Late Precambrian evolution of the Altai-Sayan folded area. In the Riphean-Vendian this region represented an island-arc stage of active margin development, which terminated after the accretion of terranes with the Siberian Craton (Berzin and Kungurtsev, 1996). The Vendian stage was marked by the deposition of thick sequences of volcanogenic-terrigenous-carbonate rocks in deep marginal seas. The clastic material of these sequences was derived from island arcs (Postnikov and Terleev, 2004).

The chondrite-normalized REE patterns in all the

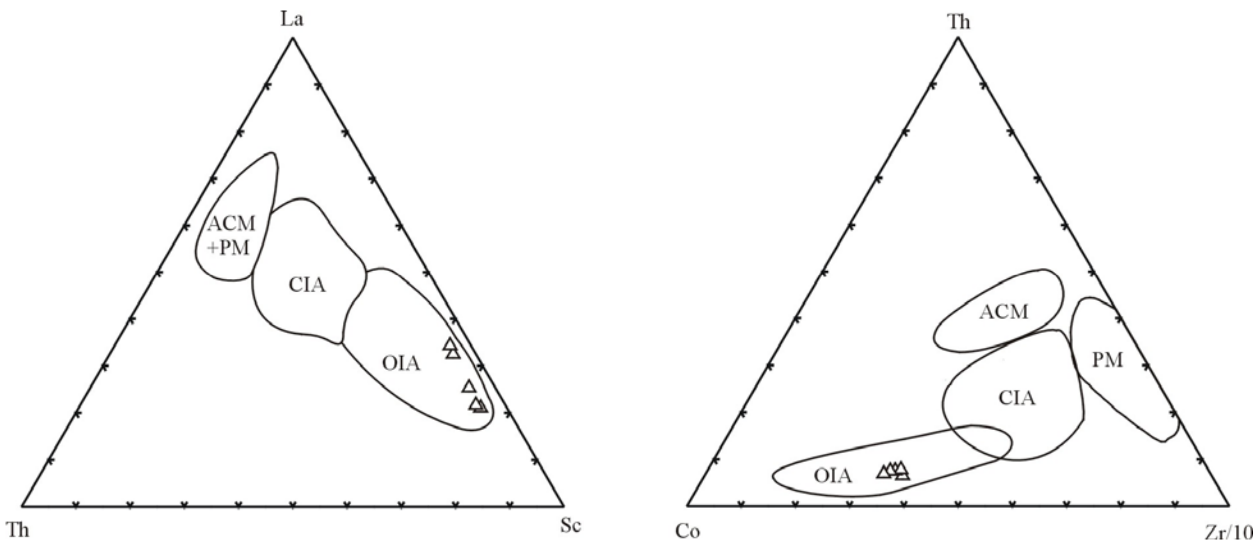


Fig. 7. Data on metapelites of the Amar Formation (open triangles) plotted in Th-Co-Zr and La-Th-Sc ternary diagrams for tectonic discrimination of graywackes (Bhatia and Crook, 1986).

ACM – active continental margin, PM – passive continental margin, CIA – continental island arc, OIA – oceanic island arc.

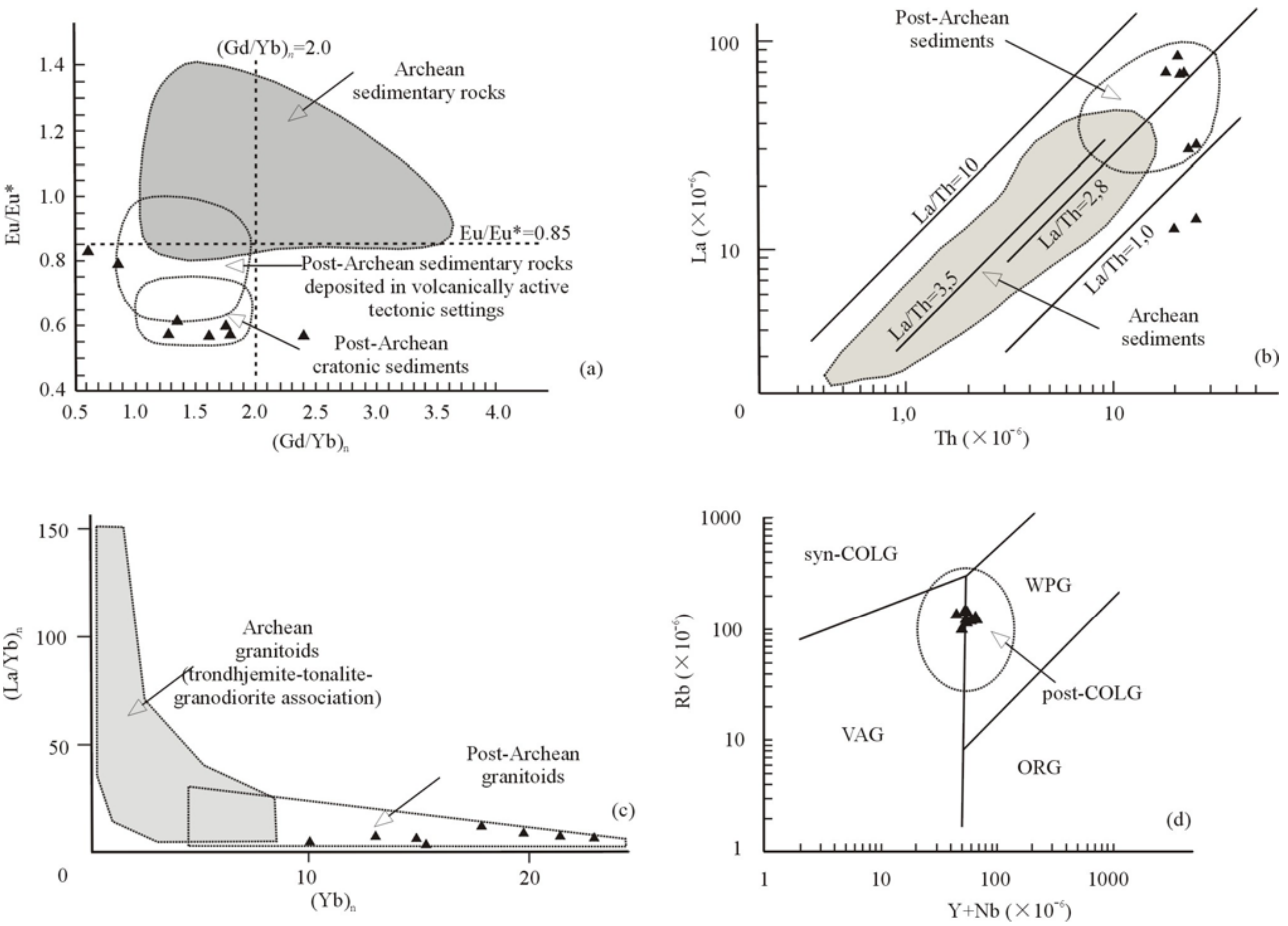


Fig. 8. Data on metapelites of the Korda Formation (black triangles) reported in the different plots and diagrams.
(a) Eu/Eu$^*$ versus $(Gd/Yb)_n$ plot (Taylor and McLennan, 1995); (b) La versus Th plot (McLennan, 1989); and (c) $(La/Yb)_n$ versus $Yb_n$ diagram for modern and Archean granitoids (Martin, 1986); (d) Rb versus (Yb + Nb) plot (Pearce et al., 1984; Pearce, 1996). The fields for the various tectonically defined granite types (d): syn-COLG and post-COLG – syn- and post-collision granites, VAG – volcanic arc granites, WPG – within plate granites, and ORG – ocean ridge granites.

studied samples of the Korda Formation (Fig. 6b) are characterized by a negative Eu anomaly (Eu/Eu$^*$ = 0.57–0.83) and higher ratios of $(La/Yb)_n$ = 2.54–17, $(Gd/Yb)_n$ = 0.61–2.39, and $(LREE/HREE)_n$ = 1.5–4.72, relative to the Amar metapelites (Table 2). These features, typical of post-Archean shales, can be attributed to the presence of erosion products of acid igneous rocks in the detritus. The formation of these products of erosion was accompanied by a decrease in the $Eu^{2+}$ content during the sedimentation of restite plagioclase (Taylor and McLennan, 1985).

Lithophile (Rb, Cs, Ba, and Sr) element concentrations in the Korda Formation metapelites are somewhat lower than in PAAS (Table 2), unlike the contents of nearly all incompatible HFSEs (Zr, Hf, Y, Ta, Th) except U. Compared to the PAAS, the group of transition metals is characterized by higher Sc contents and lower Co and Ni concentrations. The Eu/Eu$^*$ value of < 0.85 indicates a significant recycling of the older continental crust and predominance of granitoids in erosion zones (Jahn and Condie, 1995; Wronkiewicz and Condie, 1990; Podkovyrov et al., 2002; Maslov et al., 2004). The erosion of acid igneous rocks is also inferred by the higher Th/Sc (0.96–1.38) and Th/U (6.45–11.4) ratios relative to average PAAS compositions. In the Eu/Eu$^*$-$(Gd/Yb)_n$ (Taylor and McLennan, 1995) and La-Th (McLennan, 1989) diagrams, metapelite compositional data are mainly plotted in the field of the post-Archean craton deposits (Fig. 8a, b). In the $(La/Yb)_n$-$Yb_n$ diagram (Martin, 1986), all samples are clustered within the field of HREE-enriched and Co- and Ni-depleted post-Archean granitoids rather than in that of Archean acid igneous rocks (Fig. 8c). In the Rb-(Y + Nb) diagram for discriminating the tectonic setting of granites (Pearce et al., 1984; Pearce, 1996), the compositions of these rocks fall in the boundary area between volcanic-arc and within-plate granites (Fig. 8d). Intrusive complexes with similar geochemical characteristics are usually found in postcollisional geodynamic settings (Pearce, 1996). The widespread occurrence of such magmatism in the Yenisey Ridge and in neighboring regions makes this suggestion extremely plausible (Vernikovskaya et al., 2002, 2003). The high Ce/Ce* (0.77–1.25; Murray et al., 1990, 1991) and $(LREE/HREE)_n$ (1.5–4.72; Balashov, 1976) ratios suggest that the initial sediments accumulated in a shallow-water shelf setting of a continental margin under humid climate conditions which favored the intense weathering of rocks, as confirmed by the petrochemistry of rocks and lithofacies data (Akul'shina, 1980; Saraev, 1986). This conclusion is in agreement with the geological history of the Yenisey Ridge in the Precambrian: the Neoproterozoic stage of its development was preceded by the continental regime, with peneplanation and weathering crusts formation (Petrov, 1982; Nozhkin et al., 2003). The Early-Late Precambrian boundary corresponded to the subplatform regime, with accumulation of Fe- and Al-rich deposits of Korda Formation in shallow-water basins which were presumably derived from erosion products of post-Archean (c. 1750 Ma) granitoid rocks (Nozhkin et al., 2003; Postel'nikov, 1990).

## 5 Specific Behavior of REEs during Metamorphism

The Amar metapelites that underwent thermal metamorphism show no significant variations in REE contents and in their distribution pattern toward the intrusive contact (i.e. with increasing temperatures). This suggests that overall REE patterns are preserved throughout the various degrees of metamorphism and may reflect those of the protolith. This result also implies that there is no significant mass-transfer of REEs during contact metamorphism at temperatures range from 430 to 640 °C (Fig. 6a). The distribution of REEs in metapelites of the Korda Formation, which were affected by a gradual increase in pressure during collisional metamorphism, is rather differentiated (Fig. 6b). The rocks farthest from the thrust fault (zones I and II) experienced low pressures (0.35 – 0.5 GPa) and are characterized by high LREE and HREE contents, total REE contents of 303–377 ppm, maximum values of $(La/Yb)_n$ = 10.54–16.98, $(Gd/Yb)_n$ = 1.63–2.39, and $(LREE/HREE)_n$ = 3.08–4.72; in PAAS these parameters are respectively equal to 184 ppm, 9.16, 1.34, and 3.27 (Taylor and McLennan, 1985). The rocks from zones III and IV, adjacent to the Panimba thrust, formed under relatively high pressures (0.55 – 0.67 GPa). With respect to the metapelites of the previous zones and the PAAS, these rocks are greatly depleted in light and heavy REEs, with total REE contents of 80–169 ppm. Accordingly, they have low $(La/Yb)_n$ = 2.54–7.79, $(Gd/Yb)_n$ = 0.61–1.34, and $(LREE/HREE)_n$ = 1.5–2.95. Figure 6b shows that the REE patterns of two groups of these rocks are very similar in form and slope but have different abscissas. This implies that the REEs were mobilized during collisional metamorphism but had moved coherently. Such REE patterns can be related either to the removal of REEs by a metamorphic fluid phase as pressure increased under rock dehydration conditions or to a change in the chemistry of the rock protolith. Our previous studies on these rocks (Likhanov et al., 2004; Likhanov and Reverdatto, 2002) found that the prograde evolution of chemical and modal compositions of minerals during metamorphism was controlled by gradually increasing pressure (at nearly constant temperatures) accompanied by deformation within the bulk composition of the protolith. Based on the major elements distribution, we used a mass balance approach, coupled with an analysis of precision, to evaluate the net mass balance resulting from diffusion-controlled metamorphic reactions in metapelites. The calculated net mass balance is consistent with limitations imposed by rock microstructures, mineral assemblages and mineral abundances, where the growth of kyanite, staurolite, garnet, biotite, plagioclase and quartz is accompanied by decreasing amounts of chloritoid, chlorite, andalusite and muscovite. The major element distribution reflects the mineralogy of these rocks, which are mainly composed of different quantitative proportions of quartz and other minerals. Quartz, the most abundant mineral in these rocks, usually has a very low total REEs content, and REEs preferentially concentrate in other rock-forming minerals. Variations in the modal abundances of REE-free quartz and other REE-concentrated minerals could thus alter the REEs content of a rock (Cullers et al., 1997; Sifeta et al., 2005; Lopez et al., 2005). Some differences in the REE abundances of these rocks may be in part due to the mineral reactions responsible for the appearance/disappearance of minerals and for changes in mineral chemistry (Alirezaei and Cameron, 2002; Bea and Montero, 1999; Brunsmann et al., 2001). This is confirmed by mineral abundances in thin sections, where a decrease in the number of REE-concentrating minerals is accompanied by a simultaneous increase in the amount of quartz: from 35.2 vol% in zone I to 51.74 vol% in zone IV (Likhanov and Reverdatto, 2002). The reliability of calculations is also supported by the comparison of calculated mineral volume ratios from reaction equations with actual phase volumes in the rock calculated from whole-rock chemical compositions. Volume ratios in the newly formed minerals are comparable with the actual volume ratios in the rock, and quantitative ratios between the reactants and products of reactions are satisfactory (less than 20% deviation). Deviations can be explained by slight differences in bulk composition, by errors in molar volume values for minerals of variable composition, and by analytical uncertainty and mineral heterogeneity. It should be noted that these circumstances probably contribute significantly to differences in the REEs content of outer and inner zones and also contribute to the REEs budget. However, variations in REE contents from outer to inner zones are too great to be solely ascribed to reactions that occurred during metamorphism. Hence, the coherent mobility of REEs during collisional metamorphism may be attributed both to mineral reactions responsible for modal changes imprinted by metamorphism as well as to local chemical heterogeneity inherited from the initial protolith. In order to precisely estimate REEs mobility during metamorphism, calculation of the REEs budget should involve an evaluation of REE contents in coexisting minerals and mass balance estimation of modal proportions. In the field of metamorphic petrology such investigations are in their infancy (e.g. Mulrooney and Rivers, 2005).

## 6 Conclusions

Major, trace and rare earth element contents of Fe- and Al-rich metapelites from the Korda (Yenisey Ridge) and Amar (Kuznetsk Alatau) formations were determined to examine the composition and nature of their protoliths. Geochemical data, coupled with a mass balance approach applied to bulk rock chemical data, were used to estimate the REE patterns as a function of the modal rock composition and P-T conditions under which the rock evolved.

1. Fe- and Al-rich pelitic schists whose metamorphism leads to the stability of rare mineral assemblages with the participation of chloritoid, Fe-cordierite and other minerals, were the redeposited and metamorphosed products of Precambrian kaolinitic (rather than the previously-supposed lateritic) weathering crusts. During the Mesoproterozoic (Middle Riphean) and Neoproterozoic (Vendian), the chemical weathering of rocks in Kuznetsk Alatau and the Yenisey Ridge did not reach the lateritization stage with the final formation of decomposition products of aluminosilicates. Weathering was mainly limited by the predominant formation of kaolinite-montmorillonite-chlorite-hydromica rocks.

2. The geochemical distinction between the studied metapelites may have been caused by different weathering conditions in source area and tectonic settings. The protolith of the Korda Formation metapelites was produced by the erosion products of post-Archean granitoid rocks, which accumulated under humid climate conditions in shallow-water basins along the continental margin. The geochemical characteristics of the deeper primary deposits of the Amar Formation suggest that volcanic material of mafic composition derived from an island-arc environment played an important role in supplying the erosion zone. These results agree with lithofacies data and with geodynamic reconstructions of the evolution of geological complexes of the Yenisey Ridge and Kuznetsk Alatau during the Mesoproterozoic (Middle Riphean) and Neoproterozoic (Vendian), respectively.

3. The REE patterns of hornfelses suggest that increasing temperatures from 430 to 640 °C during contact metamorphism do not induce REE mobility. The coherent mobility of REEs during collisional metamorphism may be attributed both to metamorphic mineral reactions responsible for modal changes and to local chemical heterogeneity inherited from the initial protolith.

## Acknowledgements

The Russian Foundation for Basic Research (grant 06-05-64676) provided the first author with financial support. Research was also funded by the President of the Russian Federation for Support of Leading Scientific Schools (grant SS - 4922.2006.5). The authors are greatly indebted to O. Rosen and an anonymous reviewer for their thorough and constructive reviews that helped to significantly improve the quality of the original manuscript. A. Palladino is thanked for significantly improving the scientific content as well as the English.

Manuscript received Oct. 17, 2006
accepted March 15, 2007
edited by Xie Guanglian

### References

Ague, J.J., 1991. Evidence for major mass transfer and volume strain during regional metamorphism of pelites. *Geology*, 19: 855–858.

Akul'shina, E.P., 1980. Evolution of conditions of weathering and sedimentation in the Riphean and Phanerozoic of the Siberian Platform, its framing, and West Siberian Plate. In: Kazansky, Yu.P. (ed.), *Comparative Analysis of Marine Sedimentation in the Precambrian and Paleozoic*. Novosibirsk: Nauka, 101–125 (in Russian).

Alirezaei, S., and Cameron, E.M., 2002. Mass balance during dabbro-amphibolite transition, Bamble sector, Norway: implications for petrogenesis and tectonic setting of the gabbros. *Lithos*, 60: 21–45.

Balashov, Yu.A., 1976. *Geochemistry of rare-earth elements*. Moscow: Nauka, 266 (in Russian).

Bea, F., and Montero, P., 1999. Behavior of accessory phases and redistribution of Zr, REE, Y, Th, and U during metamorphism and partial melting of metapelites in the lower crust: an example from the Kinzigite Formation of Ivrea-Verbano, NW Italy. *Geochim. Cosmochim. Acta*, 63: 1133–1153.

Berzin, N.A., and Kungurtsev, L.V., 1996. Geodynamic interpretation of Altai-Sayan geological complex. *Russian Geology and Geophysics*, 37: 56–73.

Bhatia, M.R., and Crook, K.A.W., 1986. Trace element characteristics of graywackes and tectonic setting discrimination of sedimentary basins. *Contrib. Mineral. Petrol.*, 92: 181–193.

Brunsmann, A., Franz, G., and Erzinger, J., 2001. REE mobilization during small-scale high-pressure fluid-rock interaction and zoisite/fluid partitioning of La to Eu. *Geochim. Cosmochim. Acta*, 65: 559–570.

Cerny, P., Fryer, B.J., Longsstaffe, F.J., and Tammemagi, H.Y., 1987. The Archean Lac du Bonner batholith, Manitoba: igneous history, metamorphic effects, and fluid overprinting. *Geochim. Cosmochim. Acta*, 51: 1153–1177.

Condie, K.C., 1993. Chemical composition and evolution of the upper continental crust: contrasting results from surface samples and shales. *Chem. Geol.*, 104: 1–37.

Cox, R., and Lowe, D.R., 1995. Controls on sediment composition on a regional scale: a conceptual review. *J. Sediment. Res.*, A65: 1–12.

Cox, R., Lowe, D.R., and Cullers, R.L., 1995. The influence of sediment recycling and basement composition on evolution of mudrock chemistry in southwestern United States. *Geochim. Cosmochim. Acta*, 59: 2919–2940.

Cullers, R.L., Bock, B., and Guidotti, C., 1997. Elemental distributions and neodymium isotopic compositions of Silurian metasediments, western Maine, USA: Redistriburion of the rare earth elements. *Geochim. Cosmochim. Acta,* 61: 1847–1861.

Dazenko, V.M., 1984. *Granitoid Magmatism of the South-West Edge of the Siberian Platform.* Novosibirsk: Nauka, 235 (in Russian).

Dobretsov, N.L., 1974. *Glaucophane and Eclogite-Blueschist Complexes of the USSR*. Novosibirsk: Nauka, 429 (in Russian).

Fedo, C.M., Nesbitt, H.W., and Young, G.M., 1995. Unraveling the effects of potassium metasomatism in sedimentary rocks and paleosoils, with implications for paleoweathering conditions and provenance. *Geology*, 23: 921–924.

Franceschelli, M., Puxeddu, M., and Gattiglio, M., 2003. Geochemistry and origin of chloritoid schists from the Alpi Apuane, Italy: evidence of a prevailing lateritic signature. *Eur. J. Mineral.*, 15: 575–588.

Golovenok, V.K., 1977. *Precambrian High-Al Formations.* Leningrad: Nedra, 268 (in Russian).

Grauch, R.I., 1989. Rare earth elements in metamorphic rocks. In: Lipin, B.R., and McKay, G.A. (eds.), *Geochemistry and Mineralogy of Rare Earth Elements*. Washington D.C.: Mineral. Soc. Am., 147–167.

Harnois, L., 1988. The CIW index: a new chemical index of weathering. *Sediment. Geol.*, 55: 319–322.

Holail, H.M., and Moghasi, A.-K.M., 1998. Provenance, tectonic settings and geochemistry of greywackes and siltstones of the Late Precambrian Hammamat Group, Egypt. *Sediment. Geol.*, 116: 227–250.

Hoschek, G., 1969. The stability of staurolite and chloritoid and their significance in metamorphism of pelitic rocks. *Contrib. Mineral. Petrol.*, 22: 208–232.

Jahn, B.M., and Condie, K.C., 1995. Evolution of the Kaapvaal Craton as viewed from geochemical and Sm-Nd isotopic analyses of intracratonic pelites. *Geochim. Cosmochim. Acta,* 59: 2239–2258.

Kolobov, V.Y., Likhanov, I.I., and Reverdatto, V.V., 1992. Contact-metamorphic rocks. In: Dobretsov, N.L. (ed.), *Classification and Nomenclature of Metamorphic Rocks*. Novosibirsk: Nauka, 77–97 (in Russian).

Korobeinikov S.N., Polyansky O.P., Likhanov I.I., Sverdlova V.G., and Reverdatto V.V., 2006. Mathematical modeling of overthrusting as a cause of andalusite–kyanite metamorphic zoning in the Yenisei Ridge. *Transactions (Doklady) Earth Sciences*, 408: 652–657.

Kretz, R., 1983. Symbols for rock-forming minerals. *Am. Mineral.*, 68: 277–279.

Lee, Y.I., 2002. Provenance derived from the geochemistry of late Paleozoic-early Mesozoic mudrocks of the Pyeongan Supergroup, Korea. *Sediment. Geol.*, 149: 219–235.

Likhanov, I.I., 1988a. Chloritoid, staurolite and gedrite of the high -alumina hornfelses of the Karatash pluton. *Intl. Geol. Rev.*, 30: 868–877.

Likhanov, I.I., 1988b. Evolution of chemical composition of metapelite minerals during low-grade contact metamorphism. *Intl. Geol. Rev.*, 30: 878–887.

Likhanov, I.I., 1989. Metamorphic fluid composition gradients in metapelitic hornfelses. *Geochem. Intl.*, 26: 132–137.

Likhanov, I.I., 2003a. Mineral reactions in high-alumina ferriferous metapelitic hornfelses: the problem of stability of rare parageneses of contact metamorphism. *Russian Geology and Geophysics*, 44: 305–316.

Likhanov, I.I., 2003b. *Mineral Reactions and Mass Transfer during Low- and Medium-pressure Metamorphism*. Doctor of Sciences Thesis. Novosibirsk: Geo Press, 38 (in Russian).

Likhanov, I.I., Kozlov, P.S., Popov, N.V., Reverdatto, V.V., and Verschinin, A.E., 2006. Collision metamorphism induced by the overthrusts in the Transangarian part of the Yenisey Ridge. *Transactions (Doklady) Earth Sciences*, 411: 1875–1879.

Likhanov, I.I., Kozlov, P.S., Polyansky, O.P., Popov, N.V., Reverdatto, V.V., Travin, A.V., and Verschinin A.E., 2007. Neoproterozoic Age of Collisional Metamorphism in the Transangara Region of the Yenisei Ridge (based on $^{40}Ar/^{39}Ar$ Data). *Transactions (Doklady) Earth Sciences*, 413: 234–238.

Likhanov, I.I., Polyanskii, O.P., Kozlov, P.S., Reverdatto, V.V., Vershinin, A.E., Krebs, M., and Memmi, I., 2000. Replacement of andalusite by kyanite with increasing pressure at a low geothermal gradient in metapelites of the Enisei Ridge. *Transactions (Doklady) Earth Sciences*, 375: 1411–1416.

Likhanov, I.I., Polyanskii, O. P., Reverdatto, V.V., Kozlov, P.S., Vershinin, A.E., Krebs, M., and Memmi, I., 2001a. Metamorphic evolution of high-alumina metapelites near the Panimba overthrust (Yenisei Range): mineral associations, P-T conditions and tectonic model. *Russian Geology and Geophysics*, 42: 1138–1154.

Likhanov, I.I., Polyanskii, O.P., Reverdatto, V.V., and Memmi, I., 2004. Evidence from Fe-and Al-rich metapelites for thrust loading in the Transangarian region of the Yenisey Ridge, Eastern Siberia. *J. Metamorphic Geol.*, 22: 743–762.

Likhanov, I.I., and Reverdatto, V.V., 2002. Mass transfer during andalusite replacement by kyanite in Al- and Fe-rich metapelites in the Yenisei Range. *Petrology*, 10: 479–494.

Likhanov, I.I., and Reverdatto, V.V., 2004. Petrogenetic grid for ferruginous-aluminous metapelites in the $K_2O$-FeO-MgO-$Al_2O_3$-$SiO_2$-$H_2O$ system. *Transactions (Doklady) Earth Sciences*, 394: 46–49.

Likhanov, I.I., and Reverdatto, V.V., 2005. Mineral equilibria and P-T diagram for Fe- and Al-rich metapelites in the system KFMASH ($K_2O$-FeO-MgO-$Al_2O_3$-$SiO_2$-$H_2O$). *Petrology*, 13: 73–84.

Likhanov, I.I., Reverdatto, V.V., Sheplev, V.S., Verschinin, A.E., and Kozlov, P.S., 2001b. Contact metamorphism of Fe- and Al-rich graphitic metapelites in the Transangarian region of the Yenisey Ridge, eastern Siberia, Russia. *Lithos*, 58: 55–80.

Likhanov, I.I., Reverdatto, V.V., and Verschinin, A.E., 2005. Geochemistry and nature of the protolith of ferruginous-aluminous metapelites in Kuznetsk Alatau. *Transactions (Doklady) Earth Sciences*, 405: 1186–1190.

Likhanov, I.I., Sheplev, V.S., Reverdatto, V.V., and Kozlov, P.S., 1998. Contact metamorphism of ferruginous metapelites at high pressure in the Trans-Angara Region, Yenisei Range. *Transactions (Doklady) Earth Sciences*, 363: 1107–1111.

Likhanov, I.I., Sheplev, V.S., Reverdatto, V.V., Kozlov, P.S., and Kireev, A.D., 1999. The isochemical nature of the contact metamorphism of high-alumina metapelites in the Ayakhta granitoid massif, Yenisei Range. *Russian Geology and Geophysics*, 40: 91–98.

Lopez, J.M.G., Baulus, B., Fernandez-Nieto, C., and Oliete, A.Y., 2005. Factors controlling the trace-element distribution in fine-grained rocks: the Albian kaolinite-rich deposits of the Oliete Basin (NE Spain). *Chem. Geol.*, 214: 1–19.

Martin, H., 1986. Effect of stepper Archean geothermal gradients on geochemistry of subduction-related magmas. *Geology*, 14: 753–756.

Maslov, A.V., Krupenin, M.T., and Ronkin, Yu.L., 2004. Fine-grained aluminosilicate clastics of the Middle Riphean stratotype section of the South Urals: specific character of formation, composition, and evolution of sourcelands. *Lithology and Mineral Resources*, 4: 414–441 (in Russian).

McLennan, S.M., 1989. Rare earth elements in sedimentary rocks: influence of provenance and sedimentary processes. In: Lipin, B.R., and McKay, G.A. (eds.), *Geochemistry and Mineralogy of Rare Earth Elements.* Washington D.C.: Mineral. Soc. Am., 169–200.

McLennan, S.M., Hemming, S.R., Taylor, S.R., and Eriksson, K.A., 1995. Early Proterozoic crustal evolution: geochemical and Nd-Pb isotopic evidence from metasedimentary rocks, southwestern North America. *Geochim. Cosmochim. Acta,* 59: 1153–1177.

Meschide, M.A., 1986. A method of discriminating between different types of mid ocean ridge basalts and continental tholeiites with the Nb-Zr-Y diagram. *Chem. Geol.*, 56: 207–218.

Mulrooney, D., and Rivers, T., 2005. Redistribution of the rare-earth elements among coexisting minerals in metamorphic rocks across the epidote-out isograd: an example from the St. Anthony Complex, northern Newfoundlend, Canada. *Can. Mineral.*, 43: 263–294.

Murray, R.W., Buchholtz ten Brink, M.R., and Brumsack, H.J., 1991. Rare earths elements in Japan Sea sediments and diagenetic behaviour of $Ce/Ce^*$: results from ODP Leg 127. *Geochim. Cosmochim. Acta*, 55: 2453–2466.

Murray, R.W., Buchholtz ten Brink, M.R., and Jones, D.L., 1990. Rare earths elements as indicator of different marine depositional environments in chert and shale. *Geology*, 18: 268–271.

Nasedkina, V.Kh., 1981. High-Al rocks of the Bely Iyus River basin. In: Chaykovsky, V.K. (ejd.), *Mineral Deposits in Sedimentary Rocks.* Moscow: Nauka, 80–100 (in Russian).

Nesbitt, H.W., and Young, G.M., 1982. Early Proterozoic climates and plate motions inferred from major element chemistry of lulites. *Nature*, 299: 715–717.

Nozhkin, A.D., Turkina, O.M., and Bobrov, V.A., 2003. Radioactive and rare-earth elements in metapelites as an indicator of composition and evolution of the Precambrian continental crust of the southwestern margin of the Siberian craton. *Transactions (Doklady) Earth Sciences*, 390: 813–817.

Pearce, J.A., Harris, N.B.W., and Tindle, A.G., 1984. Trace element discrimination diagrams for the tectonic interpretation of granitic rocks. *J. Petrol.*, 25: 956–983.

Pearce, J.A., 1996. Sources and settings of granitic rocks. *Episodes*, 19: 120–125.

Petrov, V.G., 1982. *The Precambrian of the Western Framing of the Siberian Platform*. Novosibirsk: Nauka, 206 (in Russian).

Podkovyrov, V.N., Kovach, V.P., and Kotova, L.N., 2002. Clay deposits of the Siberian hypostratotype in the Riphean and Vendian: chemical composition, Sm-Nd systematics of sources, and steps of evolution. *Lithology and Mineral Resources*, 4: 397–418 (in Russian).

Podporina, E.K., 1985. *Rare-earth Elements in Crusts of Weathering*. Moscow: Nauka, 126 (in Russian).

Postel'nikov, E.S., 1990. Upper Proterozoic structures and formations of the eastern slope of the Yenisei Ridge. *Bull. MOIP*, 37: 14–31 (in Russian).

Postnikov, A.A., and Terleev, A.A., 2004. Neoproterozoic stratigraphy of the Altai-Sayan Folded Area. *Russian Geology and Geophysics*, 45: 269–283.

Predovsky, A.A., 1980. *Reconstruction of Conditions of Sedimentogenesis and Volcanism in the Early Precambrian*. Leningrad: Nauka, 152 (in Russian).

Reverdatto, V.V., 1973. *The Facies of Contact Metamorphism.* Canberra: Australian National University Pub. 203, 198.

Reverdatto, V.V., and Sheplev, V.S., 1998. Geodynamic factors of metamorphism and their modeling: review and analysis of the problem. *Russian Geology and Geophysics*, 39: 1664–1677.

Rolland Y., Cox S., Boullier A.-M., Pennacchioni G., and Mancktellow N., 2003. Rare earth and trace element mobility in mid-crustal shear zones: insidhts from the Mont Blanc Massif (Western Alps). *Earth Planet. Sci. Lett.,* 214: 203–219.

Rublev, A.G., 1995. *Isotope-geochronological Study of Intrusive Complexes of Altai-Sayan Region in Central Asia.* St. Petersburg: Nauka, 102 (in Russian).

Sifeta, K., Roser B.P., and Kimura J.-K., 2005. Geochemistry, provenance, and tectonic setting of Neoproterozoic metavolcanic and metasedimentary units, Werri area, Northern Ethiopia**.** *J. African Earth Sci.,* 41: 212–234.

Saraev, S.V., 1986. Lithology and petrochemistry of Riphean clay rocks on the Yenisei Ridge. In: Kazansky, Yu.P. (ed.), *Clay Minerals in Sedimentary Rocks of Siberia*. Novosibirsk: IGG SO AN SSSR, 78–85 (in Russian).

Savko, A.D., and Dodatko, A.D., 1991. *Weathering Crusts in the Geological History of the East European Platform.* Voronezh:

VGU Press, 232 (in Russian).

Shaw, D.M., 1956. Geochemistry of pelitic rocks. Part Ш: Major elements and general geochemistry. *Geol. Soc. Am. Bull.*, 67: 913–934.

Stahle, H.J., Raith, M., Hoernes, S., and Delfs, A., 1987. Element mobility during incipient granulite formation at Kabbaldurga, southern India. *J. Petrol.*, 28: 803–834.

Symmes, G.H., and Ferry, J.M., 1992. The effect of whole-rock MnO content on the stability of garnet in pelitic schists during metamorphism. *J. Metamorphic Geol.*, 10: 221–237.

Taylor, S.R., and McLennan, S.M., 1985. *The Continental Crust: Its Composition and Evolution.* Oxford: Blackwell, 312.

Taylor, S.R., and McLennan, S.M., 1995. The geochemical evolution of the continental crust. *Rev. Geophys.,* 33: 241–265.

Thompson, Jr., J.B., 1957. The graphical analysis of mineral assemblages in pelitic schists. *Am. Mineral.*, 42: 842–858.

Urbakh, V.Y., 1964. *Biometrical Methods*. Moscow: Mir, 264 (in Russian).

Vernikovskaya, A.E., Vernikovsky, V.A., and Sal'nikova, E.B., 2003. Neoproterozoic post-collisional granitoids of the Glushikha complex, the Yenisei Ridge. *Petrology*, 11: 53–67.

Vernikovskaya, A.E., Vemikovsky, V.A., Sal'nikova, E.B., Datzenko, V.M., Kotov, A.B., Kovach, V.P., Travin, A.V., and Yakovleva, S.Z., 2002. Yeruda and Chirimba granitoids (Yenisei Ridge) as indicators of Neoproterozoic collisions. *Russian Geology and Geophysics,* 43: 245–259.

Vernon, R.H., 1976. *Metamorphic Processes. Reactions and Microstructure Development.* London: George Allen & Uhwin Ltd., 225.

Vernon, R.H., 1998. Chemical and volume changes during deformation and prograde metamorphism of sediments. In: Treloar, P.J., and O'Brien, P.J. (eds.), *What Drives Metamorphism and Metamorphic Reactions?* Geological Society of London Special Publication 138, 215–246.

Visser, J.N.J., and Young, G.M., 1990. Major element geochemistry and paleoclimatology of the Permo-Carboniferous glaciogene Dwyka Formation and post-glacial mudrocks in Southern Africa. *Paleogeogr. Paleoclimat. Paleoecol.*, 81: 49–57.

Vocke, Jr., R.D., Hanson, G.N., and Grunenfelder, M., 1987. Rare earth mobility in the Roffna Gneiss, Switzerland. *Contrib. Mineral. Petrol.*, 95: 145–154.

Volobuev, M.I., Stupnikova, N.I., Zykov, S.I., 1973. The Yenisei Ridge. In: Manujlova, M.M. (ed.), *Geochronology of the USSR, Precambrian.* Leningrad: Nedra, 189–201 (in Russian).

Wood, D.A., 1980. The application of a Th-Hf-Ta diagram to problems of tectonomagmatic classification and to establishing the nature of crustal contamination of basaltic lavas of the British Tertiary volcanic province. *Earth Planet. Sci. Lett.*, 50: 11–30.

Wronkiewicz, D.J., and Condie, K.C., 1990. Geochemistry and mineralogy of sediments from the Ventersdorp and Transvaal Supergroup, South Africa: cratonic evolution during the Early Proterozoic. *Geochim. Cosmochim. Acta*, 54: 343–354.

Yudovich, Ya.E., and Ketris, M.P., 2000. *Fundamentals of Lithochemistry.* St. Petersburg: Nauka, 479 (in Russian).

Yugster, G.P., 1961. Reduction-oxidation reactions on rock metamorphism. In: Zharikov, V.A. (ed.), *Geochemical studies*. Moscow: Nauka, 495–528 (in Russian).